JOURNAL OF MATERIALS SCIENCE 26 (1991) 5019–5024

Laser remelting of cast iron: a Mössbauer study

P. SCHAAF, V. BIEHL, U. GONSER
Universität des Saarlandes, Werkstoffwissenschaften, D-6600 Saarbrücken, FRG

M. BAMBERGER
Department of Materials Engineering, Technion, Israel Institute of Technology, Haifa 32000, Israel

Ph. BAUER
Laboratoire de physique du solide, Université de Nancy I, F-54506 Vandoeuvre Cedex, France

The Mössbauer spectroscopy in backscattering technique (CXMS) was used to analyse cw-CO_2 laser-treated samples of cast iron. The depth profile as revealed by Mössbauer phase analysis is discussed in connection with the initial microstructure.

1. Introduction

Considerable efforts have been devoted to surface hardening of iron-based alloys by means of laser irradiation [1, 2]. By controlled laser power and motion of the workpiece with respect to the incident beam, it is possible to quench either a molten layer or a solely austenitized zone of commercial steels after fast heating. In general, retained austenite with high interstitial carbon content is obtained together with more or less martensite and carbides [3–6]. Cast iron, owing to its low price, good castability and machinability, has recently attracted a good deal of interest in this special field of surface treatment. Improvement of hardness and wear resistance after laser irradiation have been reported [7–9].

In the present work we studied the phase transformations occurring during a laser treatment of three grey cast iron samples. The starting material consisted of flake and nodular graphite in a perlitic matrix and nodular graphite in a ferritic matrix, respectively. The depth profile was investigated using ^{57}Fe Mössbauer spectroscopy supplemented by metallographic and hardness data.

2. Experimental procedure

The nominal compositions of the samples used in this study are given in Table I together with the observed initial microstructure [7].

Before laser treatment, the discs of 23 mm diameter and 5 mm thickness were mechanically ground. The samples were submitted to an incident power of 700 W with a beam diameter of 200 μm under a protective argon shielding gas. Adjacent passes with 50% overlap were carried out, each with a relative velocity of 400 mm s^{-1} with respect to the incident beam [7].

TABLE I Chemical composition (wt %) and microstructure of the specimens (CE = C + 1/3 Si)

Specimen	C	CE	Mn	Si	Cr	Microstructure
A	3.40	4.00	0.59	1.80	0.18	Pearlite + flake graphite
B	3.50	4.30	0.30	2.40	–	Pearlite + nodular graphite
C	3.40	4.33	0.66	2.80	–	Ferrite + nodular graphite

Micrographs were performed after etching the cross-section of each sample in order to appreciate the magnitude of the affected zones. After electropolishing, phase identification of the treated surface was achieved by means of X-ray diffraction (XRD) and Mössbauer spectroscopy. The spectra were recorded at room temperature in the backscattering geometry by detecting the re-emitted 6.4 keV X-ray following resonant absorption. The measured area was set across several adjacent laser tracks. For details of the experimental apparatus see [10, 11].

Furthermore, in order to investigate the depth profile of the heat-affected zone, layers of material were removed mechanically. Mössbauer spectra were thus recorded at various depths and supplemented by microhardness measurements (H_V 0.1).

3. Results

The cross-section micrographs in Figs 1a–3a show evidence of phase transformations due to laser treatment with respect to the unaffected bulk zone. The overlapping laser tracks are observable. The flake graphite of Sample A (Fig. 1a) has been completely dissolved in a molten layer of about 200 μm, subsequently quenched, giving a fine ledeburite-type structure (Fig. 1b). On the contrary, for Samples B and C (Fig. 2, 3), the affected zone is martensitic down to $\approx$ 100 μm with the remaining graphite nodules incompletely dissolved during the heating process and surrounded by a kind of bright ring, attributed to retained austenite.

It is worth noting that Sample B exhibits the best wear resistance as reported by Bamberger *et al.* [7]. In Sample A, deep hot cracks were found, formed during the rapid solidification and cooling. No cracks were observable for Specimens B and C.

0022–2461/91 $03.00 + .12

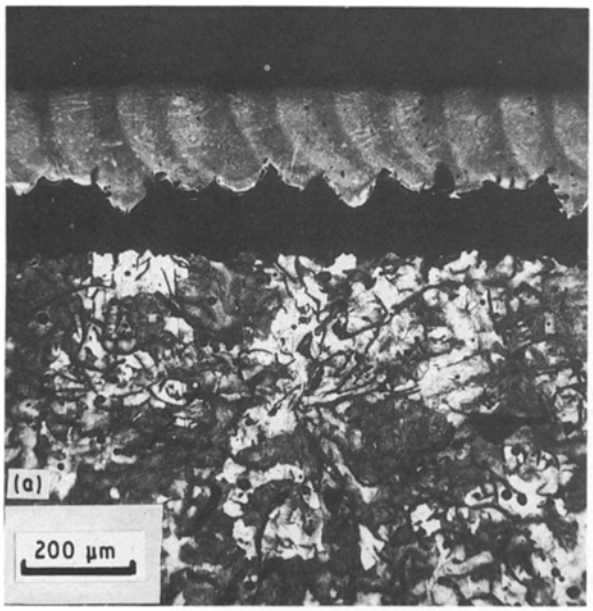

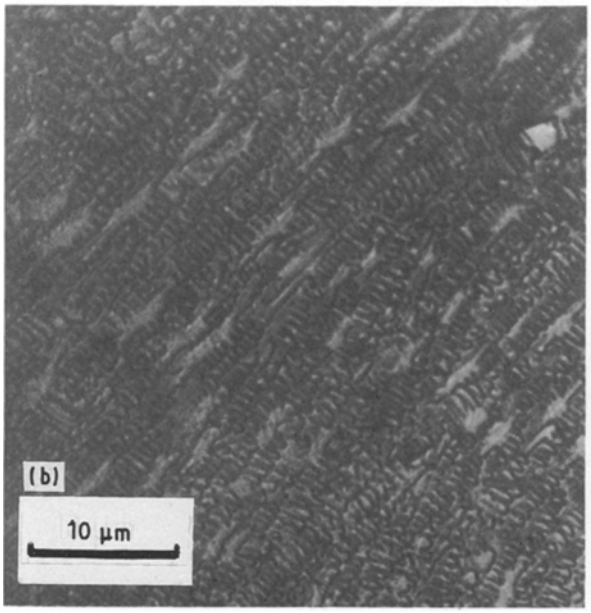

Figure 1 Cross-section micrographs of Sample A after laser treatment. (a) Low magnification, (b) high magnification, eutectic solidification in the surface of (a).

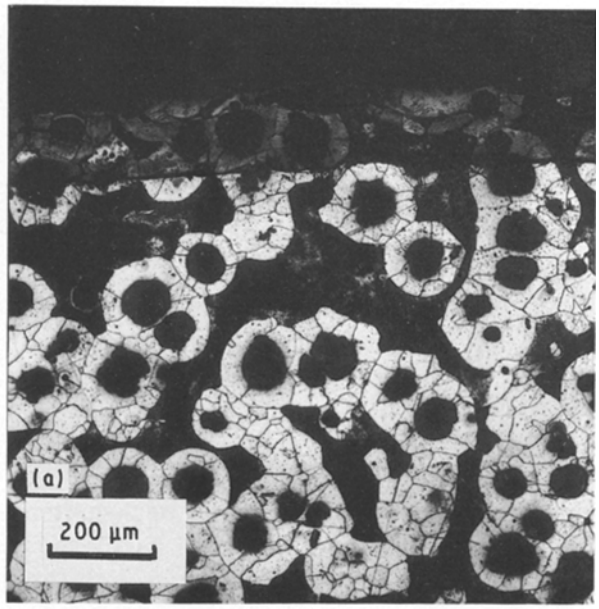

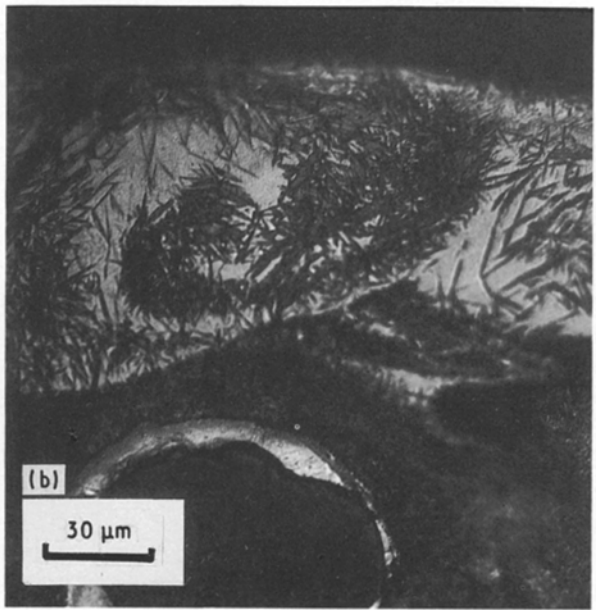

Figure 2 High and low magnification cross-section micrographs of Sample B after laser treatment.

Mössbauer spectra taken at various depths for Samples A, B and C are displayed in Figs 4–6 in comparison to those spectra corresponding to the untreated bulk. The prominent feature of the spectra corresponding to the heat-affected zones is a central paramagnetic component made of a single line plus a quadrupole split doublet. The hyperfine parameters of these lines are consistent with those of retained austenite with interstitial carbon [12, 13]. Depending on the sample and the depth investigated, the paramagnetic component is superimposed on several magnetically split subspectra which are also found in the corresponding bulk spectra.

The spectra of Sample A exhibit cementite (Fig. 4a), resolved into two sextets attributed to the inequivalent iron sites present in this component [13, 14]. At a depth of about 200 µm, sextets with larger magnetic hyperfine splitting set in. They are ascribed to iron atoms having, respectively, 0, 1 or 2 and more Si/Mn first and second nearest neighbours in the b c c structure [15] in accordance with the observed binomial distribution of their abundancies. The depletion of the hyperfine field caused by one Si/Mn neighbouring atom is in accordance with the findings of Wertheim *et al.* [16] and Bernas and Campbell [17]. In the spectra of Fig. 4c and d the reduced amount of cementite does not allow its computation with two subspectra and only a mean value for the hyperfine field was then used.

In the spectra of Samples B (Fig. 5) and C (Fig. 6) the austenite appears mixed with iron of b c t/b c c structure having the same nearest neighbour configuration as previously encountered in Sample A. It is worth noting that for Sample B the sextet relevant to

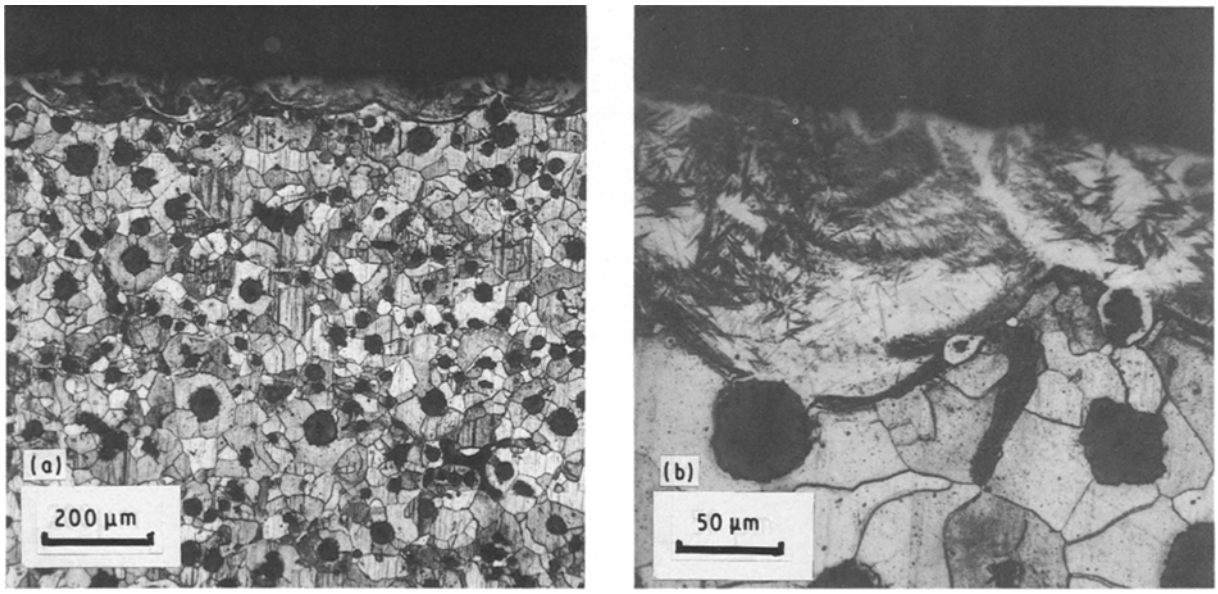

Figure 3 High and low magnification cross-section micrographs of Sample C after laser treatment.

cementite is practically absent down to 500 μm (Fig. 5d) which signals the disappearance of pearlite in the affected layer during the heating process.

Finally it is noted that the phase analysis at the surface revealed by Mössbauer spectroscopy (Figs 4a, 5a, 6a) is in accordance with XRD results [7].

4. Discussion

The depth profile as revealed by Mössbauer spectroscopy is displayed in Figs 7a, 8a and 9a where the relative abundancies of retained austenite, cementite and either annealed martensite or ferrite are plotted against the depth, together with the hardness data

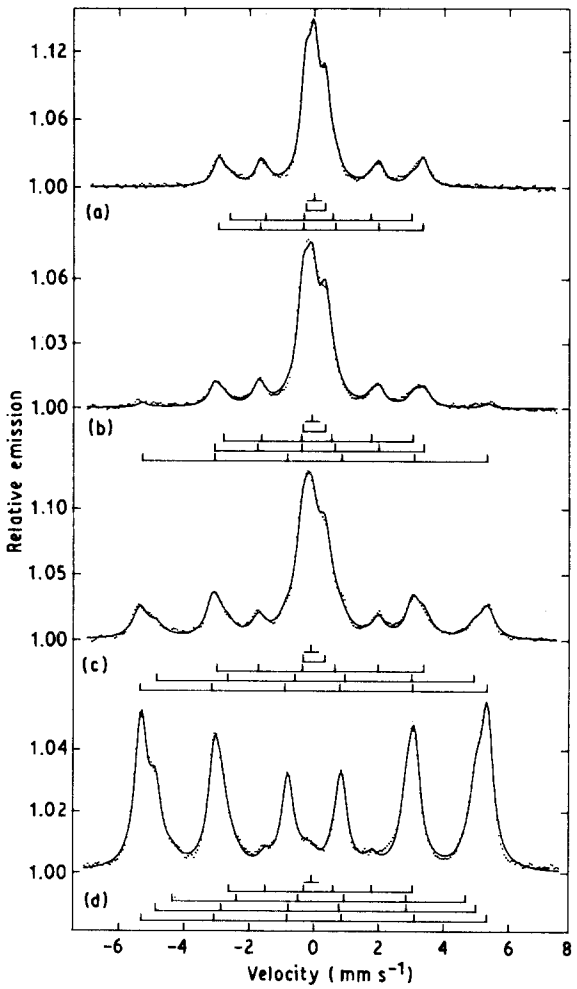

Figure 4 Mössbauer spectra of laser-treated Sample A at different depths: (a) laser-treated surface, (b) 209 μm, (c) 252 μm, (d) untreated (bulk).

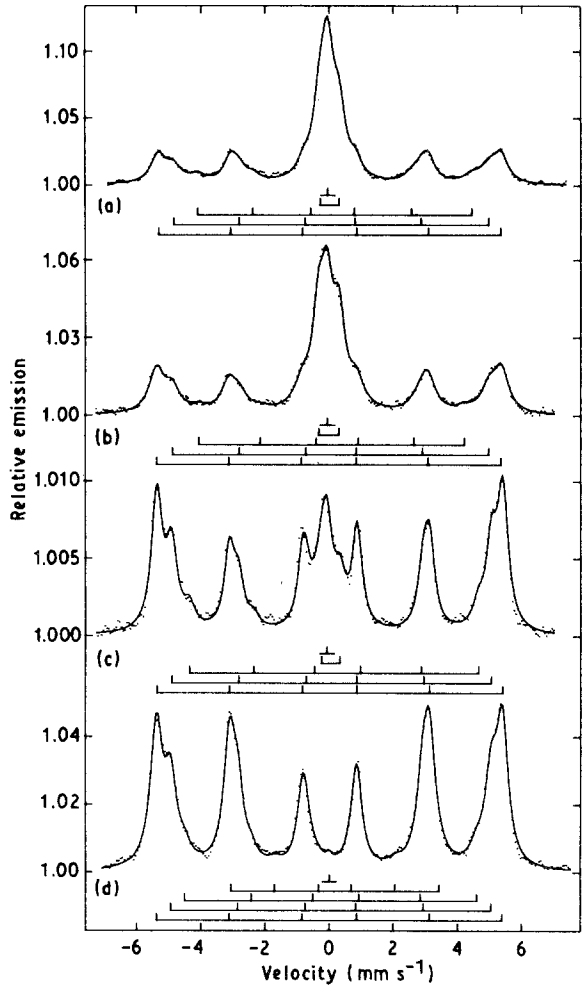

Figure 5 Mössbauer spectra of laser-treated Sample B at different depths: (a) laser-treated surface, (b) 81 μm, (c) 122 μm, (d) untreated (bulk).

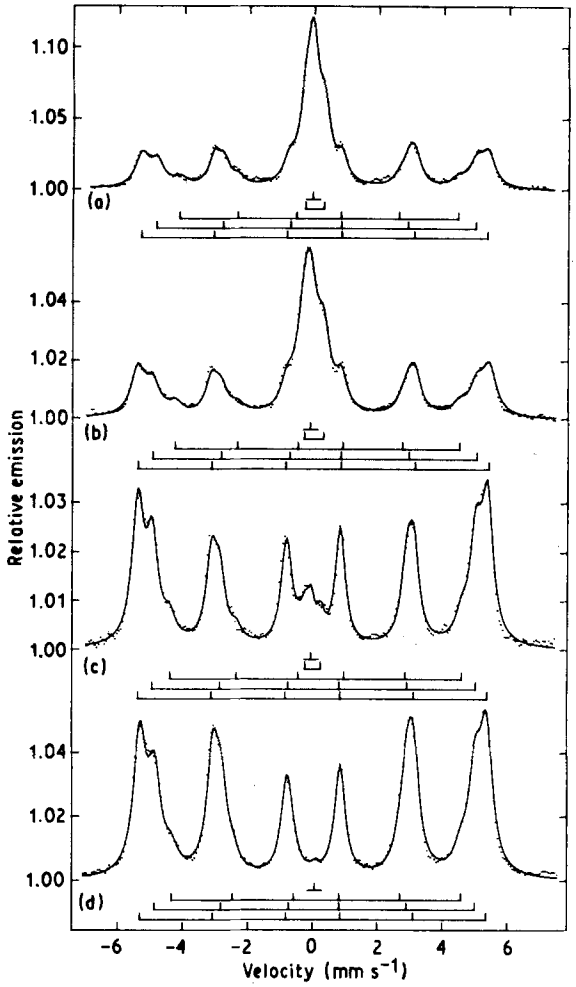

Figure 6 Mössbauer spectra of laser-treated Sample C at different depths: (a) laser-treated surface, (b) 87 μm, (c) 166 μm, (d) untreated (bulk).

(Figs 7b, 8b and 9b). The interstitial carbon content of the retained austenite, computed using the repulsive model [13], is also quoted in weight per cent.

The salient feature is a marked contrast between the depth profile obtained for Sample A and that of Samples B and C, the last two being almost alike. As mentioned earlier by Bamberger *et al.* [7], the graphite morphology of the starting material is thought to be responsible for the observed behaviour. In the following the influence of the microstructure during the fast heating prior to quenching is discussed.

The flake graphite of Sample A dissolves completely, leading to an almost uniform nearly eutectic composition, i.e. the liquid point is then reached. The subsequent quenched molten zone is made of fine ledeburite ($\gamma + Fe_3C$) where the austenite phase has a high carbon content (≈ 2.3 wt %) and can thus be retained down to room temperature, due to a lowered martensite start, M_s, temperature [2]. Adjacent reheating (annealing) of affected tracks leads to a refinement of the ledeburite structure in the overlap zone as revealed by the micrograph of Fig. 1a. Despite the fast heating and quenching process, the relative abundancies of retained austenite (62%) and precipitated cementite (38%) deduced from the Mössbauer analysis are comparable to those obtained when the

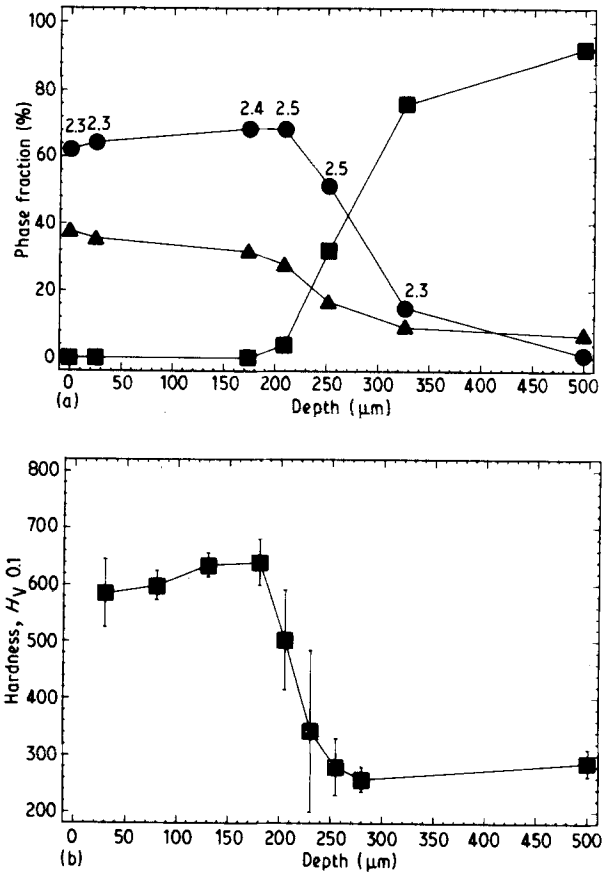

Figure 7 (a) Depth profile of laser-treated Sample A. (●) γ = austenite, (▲) C = cementite, (■) M = martensite/ferrite; the carbon concentration in austenite is indicated (wt %). (b) Variation of hardness of Sample A with depth.

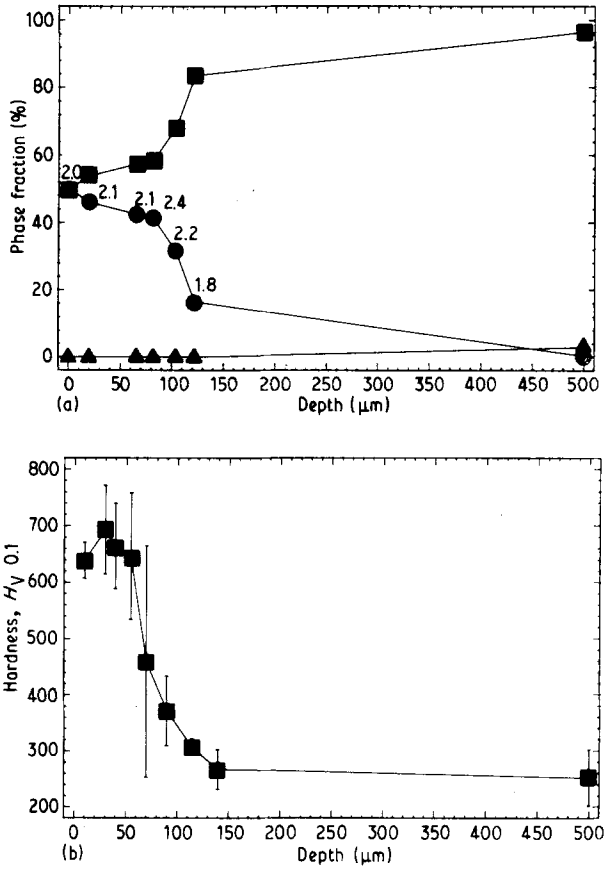

Figure 8 (a) Depth profile of laser-treated Sample B. (●) γ = austenite, (▲) C = cementite, (■) M = martensite/ferrite; the carbon concentration in austenite is indicated (wt %). (b) Variation of hardness of Sample B with depth.

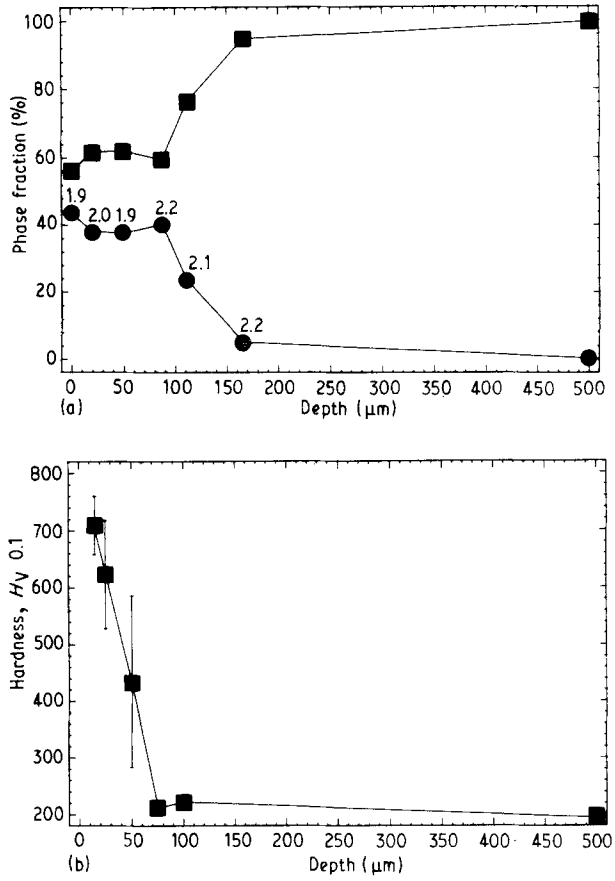

Figure 9 (a) Depth profile of laser-treated Sample C. (●) γ = austenite, (■) M = martensite/ferrite; the carbon concentration in austenite is indicated (wt %). (b) Variation of hardness of Sample C with depth.

equilibrium phase diagram is considered: 58% and 42%, respectively, computed with an equivalent carbon content of 4 wt %.

The sudden decrease in the retained austenite and cementite amounts accompanied by an increase of ferrite suggests that the extension of the quenched molten layer would be about 200 μm. One notices that the hardened zone extends almost to the same depth and is relative to the amount of cementite, i.e. ledeburite, precipitated during the cooling process.

Compared to the fine flake graphite of Sample A, the larger graphite nodules present in Samples B and C are difficult to dissolve completely. This results in two species of austenite because homogenization is far from being complete during the fast heating. In the neighbouring region of the graphite nodules, the austenite solid solution has an interstitial carbon content of 2.0–2.3 wt % and can thus be stable down to room temperature as demonstrated by the Mössbauer spectra. On the contrary, the carbon-depleted austenite zones undergo a martensitic transformation owing to a raised M_s temperature and are responsible for the observed hardness. From the Mössbauer analysis it is difficult to distinguish between ferrite and martensite, because the latter is annealed during the second heating from adjacent passes, i.e. no extra satellites due to interstitial carbon atoms are found. Going deeper into the affected zone, martensite will be mixed with more and more ferrite, as is also indicated by the hardness data, accompanied by decreasing austenitizing time and temperature. Finally, it is worth noting that in case of Sample B, for which cementite is completely dissolved during the fast heating, the cooling rate is high enough to avoid any new precipitation of this phase. This results in a somewhat higher fraction of retained austenite and a stabilization of the martensite content down to 50 μm, in comparison with Sample C, for which the hardness decreases more rapidly.

5. Conclusion

Grey cast-iron specimens subjected to laser remelting are examined by means of backscattered Mössbauer spectra at room temperature in connection with a metallographic study and hardness measurements (H_V 0.1). The starting materials are, respectively, pearlite interspersed with flake graphite, pearlite with nodular graphite and ferrite with nodular graphite, submitted to a series of overlapping passes with an incident power of 700 W. The depth profile of the phases obtained after rapid solidification is performed down to 500 μm for each sample.

The laser treatment leads to a significant increase in the surface hardness compared to that of the untreated bulk, but the depth profile observed depends strongly upon the initial graphite morphology. The flake graphite dissolves completely during the fast heating leading to a quenched molten zone resulting in a fine mixture of retained austenite and cementite. On the contrary, the presence of nodular graphite results in a solid-phase transformation leaving annealed martensite mixed with some retained austenite. The vanishing of retained austenite with high carbon content at a given depth yields the thickness of the affected layer. It is shown that Mössbauer spectroscopy performed in backscattering geometry is a powerful tool for investigation of laser-treated iron-containing samples.

Acknowledgement

This work was partly supported by the Deutsche Forschungsgemeinschaft (DFG). We thank Dr Frank Aubertin for critically reading the manuscript.

References

1. W. AMENDE, "Härten von Werkstoffen und Bauteilen des Maschinenbaus mit dem Hochleistungslaser" (VDI, Düsseldorf, 1985).
2. K. WISSENBACH, Thesis, TH Darmstadt (1985).
3. L. BLAES, Ph. BAUER, U. GONSER and R. KERN, *Z. Metallkde* **79** (1988) 278.
4. M. CARBUCICCHIO and G. PALOMBARINI, *Thin Solid Films* **126** (1985) 293.
5. P. SCHAAF, Ph. BAUER and U. GONSER, *Z. Metallkde* **80** (1989) 77.
6. R. KERN, W. A. THEINER, P. SCHAAF and U. GONSER, in "Non-destructive characterization of materials", edited by P. Höller, V. Hauk, G. Dobmann, C. O. Ruud and R. E. Green (Springer Verlag, Berlin, Heidelberg, New York, 1989) p. 598.
7. M. BAMBERGER, M. BOAS and O. AKIN, *Z. Metallkde* **79** (1988) 806.
8. H. W. BERGMANN and B. L. MORDIKE, *Z. Werkstofftech.* **14** (1983) 228.

9. A. GILLNER, K. WISSENBACH, E. W. KREUTZ, in "Laser treatment of materials", edited by B. L. Mordike (DGM Informationsgesellschaft, Oberursel, 1987) p. 213.
10. L. BLAES, H.-G. WAGNER, U. GONSER, J. WELSCH and J. SUTOR, *Hyperfine Interactions* **29** (1986) 1571.
11. P. SCHAAF, L. BLAES, J. WELSCH, H. JACOBY, F. AUBERTIN and U. GONSER, *ibid.* **58** (1990) 2541.
12. Ph. BAUER, O. N. C. UWAKWEH and J. M. R. GENIN, *Hyperfine Interactions* **41** (1988) 555.
13. M. RON, in "Applications of Mössbauer spectroscopy", Vol. II, edited by R. L. Cohen (Academic Press, New York, 1980) p. 329.
14. P. SCHAAF, S. WIESEN and U. GONSER, submitted to *Acta Metall.*
15. P. SCHAAF, Ph. BAUER and U. GONSER, *Hyperfine Interactions* **46** (1989) 541.
16. G. K. WERTHEIM, V. JACCARINO, J. H. WERNICK and D. N. E. BUCHANAN, *Phys. Rev. Lett.* **12** (1964) 24.
17. H. BERNAS and I. A. CAMPBELL, *Solid State Commun.* **4** (1966) 577.

Received 10 July 1990
and accepted 6 February 1991